High Dynamic Range Resampling for Software Radio

Arthur David Snider, Laiq Azam

Abstract—The classic problem of recovering arbitrary values of a band-limited signal from its samples has an added complication in software radio applications; namely, the resampling calculations inevitably fold aliases of the analog signal back into the original bandwidth. The phenomenon is quantified by the spur-free dynamic range. We demonstrate how a novel application of the Remez (Parks-McClellan) algorithm permits optimal signal recovery and SFDR, far surpassing state-of-the-art resamplers.

Keywords— Sampling methods, Signal sampling, Digital radio, Digital-analog conversion.

I. INTRODUCTION

THE goal of software radio is to replace electronic signal processing functions with digital signal processing algorithms. Thus the received analog signal is to be sampled and replaced by a digital signal as early as possible (that is, as close to radio frequency as possible). In any assembly of digital radio hardware the various devices for the subsequent digital processing may call for disparate sampling rates. For robustness, then, it is necessary to have an algorithm that changes the sampling rate of a discrete signal; it "fills in" or interpolates the values of the original analog signal, between samples.

A classic theorem from approximation theory, developed and refined by scientists from Poisson to Shannon $[1-7]$, states that exact interpolation is possible if the analog signal is sampled at a rate exceeding twice its bandwidth. To be precise, let $x(t)$ be an analog function with Fourier transform $X(\omega)$ confined to the interval $[-\Omega_{BW}, \Omega_{BW}]$, sampled at intervals of duration $T < \pi/\Omega_{BW}$. Then the condition

$$X(\omega) \equiv \frac{1}{2\pi} \int_{-\infty}^{\infty} x(t)\, e^{-j\omega t}\, dt \;=\; 0 \; if \; |\omega| \;>\; \Omega_{BW}$$

implies that for any time t, expressed in terms of sampling instants as $t = MT + \tau \; (0 \le t < T)$,

$$x(t) = \sum_{n=-\infty}^{\infty} x(nT)\, sinc(\frac{t}{T} - n)$$
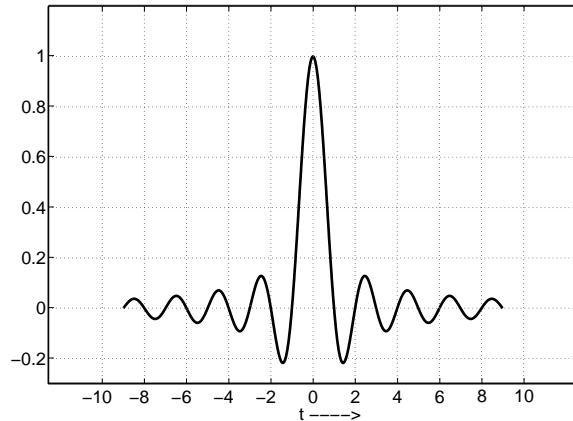$$= \sum_{n=-\infty}^{\infty} x([M-n]T)\, sinc(\tau/T \,+\, n) \tag{1}$$

Fig. 1. $sinc(t)$

The second formula emphasizes that the samples taken more remotely from the time t ($\approx MT$) are weighted less, in the reconstruction of $x(t)$ (since $sinc(\cdot)$ goes to zero at infinity; see Figure 1).

Because the support of the sinc function is of infinite extent, *exact* resampling entails using all of the sampled values $x(nT)$ and is a practical impossibility. Commercial resamplers typically replace the $sinc$ by a finitely supported function h such as a truncated $sinc$ or a linear or bicubic spline (Figure 2), giving the approximate interpolations

$$x(t) \approx \xi(t) = \sum_{supp\, h} x(nT)\, h(\frac{t}{T} - n)$$
$$= \sum_{supp\, h} x([M-n]T)\, h(\frac{\tau}{T} + n) \tag{2}$$

If the support of h has length L, (2) gives an approximate interpolation using $int(L)$ sampled values.

The figures of merit for an approximate "interpolating kernel" h are

1) the length of the support of h (the number of multiplies in (2),
2) the accuracy of the interpolation (2), and
3) the spur-free dynamic range, to be discussed in the following section.

II. SPUR-FREE DYNAMIC RANGE

The Fourier transform of equation (2) is expressed in term of the transforms $\Xi(\omega)$ of $\xi(t)$ and $H(\omega)$ of $h(t)$, respectively,
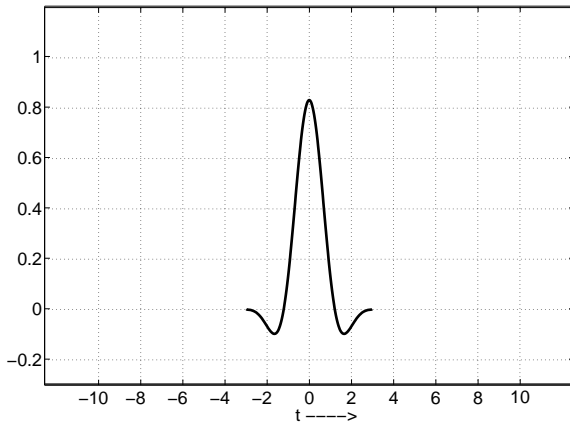
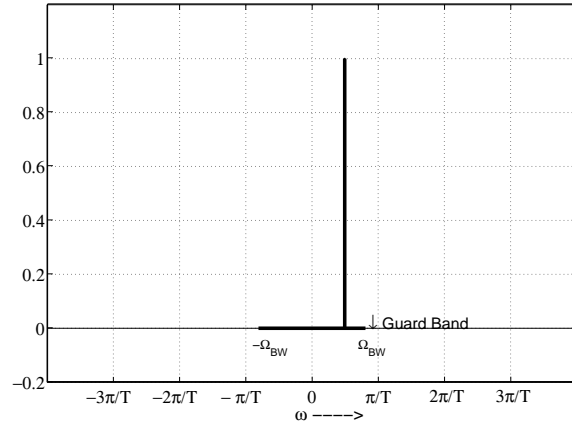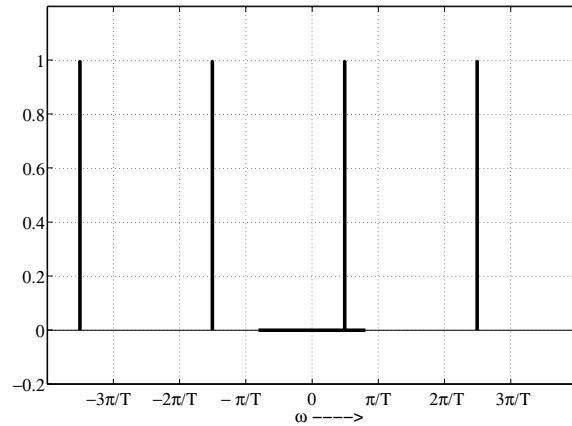Fig. 2.   Finitely supported resampler kernel

Fig. 3.   Fourier Transform of Monotone

Fig. 4.   Fourier Transform of sampled monotone

by

$$\Xi(\omega) = T \sum_{n=-\infty}^{\infty} x(nT) \; e^{-jn\omega T} H(\omega T) \qquad (3)$$

The same operation, performed on equation (1), expresses the Fourier transform $X(\omega)$ of $x(t)$ in terms of the transform of $sinc(t)$, which is the characteristic function $\chi_{\pm\pi}(\omega)$ of the interval $(-\pi, \pi)$ ($= 1$ for $|\omega| < \pi$, zero otherwise), divided by 2π:

$$
\begin{aligned}
X(\omega) &= \frac{T}{2\pi} \sum_{n=-\infty}^{\infty} x(nT) \; e^{-jn\omega T} \; \chi_{\pm\pi}(\omega T) \\
&= \left(\frac{T}{2\pi} \sum_{n=-\infty}^{\infty} x(nT) \; e^{-jn\omega T} \right) \chi_{\pm\pi/T}(\omega) \qquad (4) \\
&\equiv X_{per}(\omega) \; \chi_{\pm\pi/T}(\omega)
\end{aligned}
$$

where $X_{per}(\omega)$ is the π/T-periodic extension of $X(\omega)$. Thus $(3, 4)$ become

$$
\begin{aligned}
\Xi(\omega) &= X_{per}(\omega) \; 2\pi H(\omega T) \\
X(\omega) &= X_{per}(\omega) \; \chi_{\pm\pi/T}(\omega)
\end{aligned}
\qquad (5)
$$

In software radio the interpolated function $\xi(t)$ is obviously not computed at every time t; only the discrete values called for by the application are needed. But the effect is formally equivalent to constructing and resampling $\xi(t)$, and this interpretation is used in the subsequent analysis. Typically the resampling is done at a constant rate, differing from the original rate $1/T$. (Some applications may call for resampling at the *original* rate, and some may resample ξ at nonuniform intervals.) Although the spectral aspect of resampling has been explained by other authors, for expository reasons we illustrate it for the simplest bandlimited signal, a (complex) monotone $x(t) = e^{j\Omega t}$. Figure 3 displays the Fourier transform, $X(\omega) = \delta(\omega - \Omega)$, of the monotone. It also displays the "oversampling guardband", usually expressed as a fraction of the frequency Ω_{BW}. Figure 4 displays the Fourier transform of the sampled signal $x(nT)$; the well-known "folding" effect results in the periodic $X_{per}(\omega)$.

Figure 5 displays the function $2\pi H(\omega T)$ derived from the interpolating kernel $h(t)$. If h is finitely supported, its transform must have unbounded support. Figure 6 then shows the Fourier transform $\Xi(\omega)$ of the reconstructed function $\xi(t)$. Note how the unbounded support of $H(\omega T)$ has given rise to "spurs" in the spectrum of $\xi(t)$.

Resampling $\xi(t)$ at a new rate $1/T'$ then folds these spurs into the original signal's bandwidth, as seen in Figures 7 (for $1/T' > 1/T$) and 8 (for $1/T' < 1/T$ but still faster than the critical rate Ω_{BW}/π). For the software radio application, where the bandwidth is divided among different users, this results in spectral leakage into other subbands and must be suppressed.

III. QUANTATIVE ERROR METRICS

The quality of any resampling algorithm, as regards the software radio application, is measured by the accuracy of the interpolated signal and the suppression of the spurs that are aliased into the bandwidth. For the sake of exposition we quantify the latter first.

Figure 6 shows that the transform $\Xi(\omega)$ of the interpolation $\xi(t)$ of a monotone can be envisioned as a "comb" of delta functions modulated (in frequency space!) by the envelope $2\pi H(\omega T)$. The highest amplitude that any spur can have is
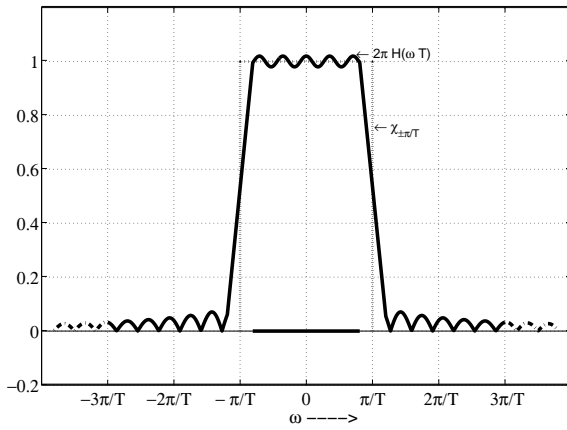
Fig. 5. $2\pi H(\omega T)$ and $\chi_{\pm\pi/T}$
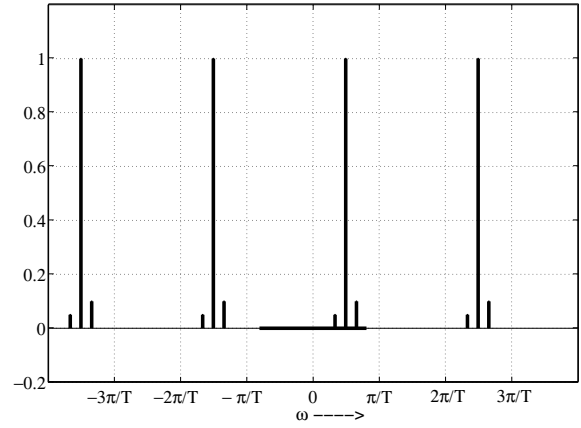
Fig. 7. Re-sampled with $T' < T$
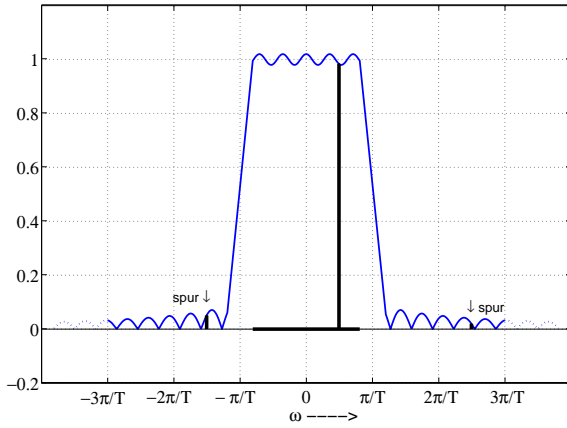
Fig. 6. $\Xi(\omega)$
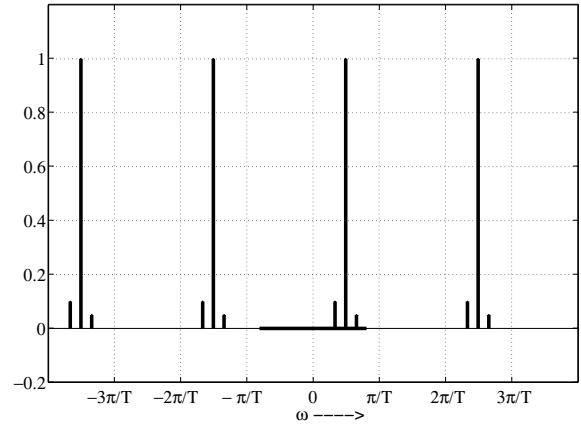
Fig. 8. Re-sampled with $T' > T$

thus limited by the maximum of $|2\pi H(\omega T)|$ in the region where the spur occurs. A little study of Figure 4 reveals that all spurs have frequencies higher than (π/T) plus the oversampling guard band $(\pi/T) - \Omega_{BW}$. Thus

$$\text{max spur} = \max\left\{ \left|2\pi H(\omega T)\right| : \frac{2\pi}{T} - \Omega_{BW} \le \omega < \infty \right\}$$

The *spur-free* dynamic range is measured by the ratio of the intensity of the original monotone (one) to the maximum spur. Thus a specification of β dB as the SFDR is satisfied by demanding:

$$\max\left\{ \left|2\pi H(\omega T)\right| : \frac{2\pi}{T} - \Omega_{BW} \le \omega < \infty \right\} \le 10^{(-\beta/20)} \quad (6)$$

Now we turn to assessing the *accuracy* of the interpolates. Observe that the difference between the actual signal value and the value computed by resampling can be expressed in terms of the Fourier transforms by:

$$x(t) - \xi(t) = \int\limits_{-\infty}^{\infty} \left\{ X(\omega) - \Xi(\omega) \right\} e^{j\omega t} d\omega$$

$$= \int\limits_{-\infty}^{\infty} X_{per}(\omega) \left[\chi_{\pm\pi/T}(\omega) - 2\pi H(\omega T)\right] e^{j\omega T} d\omega$$

Therefore the mean square (L^2) energy of the interpolation error can be measured by Parsevals' theorem:

$$\text{error energy} = \|x(t) - \xi(t)\|_2^2 = 2\pi \int\limits_{-\infty}^{\infty} \left\{ |X_{per}(\omega)|^2 \right.$$
$$\left. |\chi_{\pm\pi/T}(\omega) - 2\pi H(\omega T)|^2 \right\} d\omega$$

This error is estimated by quantifying the difference between $\chi_{\pm\pi/T}(\omega)$ and $2\pi H(\omega T)$. If we assume that the SFDR is large, then $\chi_{\pm\pi/T}(\omega)$ and $2\pi H(\omega T)$ are both negligible for $|\omega| > 2\pi/T - \Omega_{BW}$, while $X_{per}(\omega) = 0$ for $\Omega_{BW} < |\omega| < 2\pi/T - \Omega_{BW}$; therefore the error energy N and the signal energy S are related by
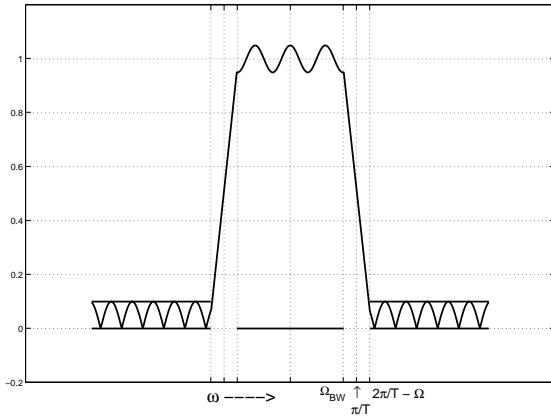
Fig. 9. $2\pi H(\omega T)$ and $\chi_{\pm\pi/T}$

$$N \approx 2\pi \int_{-\Omega_{BW}}^{\Omega_{BW}} |X_{per}(\omega)|^2 |\chi_{\pm\pi/T}(\omega) - 2\pi H(\omega T)|^2 d\omega$$

$$\leq 2\pi \int_{-\Omega_{BW}}^{\Omega_{BW}} |X_{per}(\omega)|^2 d\omega \cdot \qquad (7)$$

$$\cdot \max_{|\omega| \leq \Omega_{BW}} \{|\chi_{\pm\pi/T}(\omega) - 2\pi H(\omega T)|^2\}$$

$$= S \times \max_{|\omega| \leq \Omega_{BW}} \{|\chi_{\pm\pi/T}(\omega) - 2\pi H(\omega T)|^2\}$$

Thus a specification of (minus) α dB as the maximum allowable distortion (α = signal to noise energy ratio SNR) can be satisfied by imposing the (sufficient) condition

$$\max\{|1 - 2\pi H(\omega T)|^2 \; : \; |\omega| \leq \Omega_{BW}\} \leq 10^{-\alpha/20} \qquad (8)$$

IV. SOLUTION

The constraints $(6, 8)$ are suggestive of the classic application of the Parks-McClellan coding of Remez's exchange algorithm, whereby one seeks a digital filter with specified passband and stopband amplitudes, separated by a don't-care band. See Figure 9. However, the situation is different here. We are looking for a *continuous finitely-supported* function $h(t)$ whose Fourier transform $H(\omega)$ has these specifications.

The *modus operandi* by which we jury-rig the Parks-McClellan algorithm to solve our problem is to consider the Riemann sum interpretation of the integral arising in the Fourier transform: if $h(t)$ is tabulated with the mesh points $t_n = n\,\Delta t$ and we introduce the abbreviation $\nu = \Delta t\,\omega$,

$$H(\omega) = \frac{1}{2\pi} \int h(t)e^{-j\omega t}dt \approx \frac{1}{2\pi} \sum h(t_n)e^{-jt_n\omega}\Delta t$$

$$= \sum [h(n\Delta t)\frac{\Delta t}{2\pi}]e^{-jn\Delta t\omega} \quad \equiv \quad \sum \eta_n e^{-jn\nu}$$

where $\eta_n = h(n\Delta t)\,\Delta t/2\pi$. The final member of this equation is a trigonometric polynomial; but its degree is enormous - namely, the number of discretization points required to tabulate the kernel $h(t)$.

In theory, at least, one can specify the degree (= [length of support of $h]\div\Delta t$), interpret ν as the "frequency", specify $[0, \Omega_{BW}\Delta t]$ and $[2\pi\Delta t/T - \Omega_{BW}\Delta t, \infty)$ respectively, as the passband and stopband, and toy with the stopband and passband weights until the specifications $(6, 8)$ are met. Multiplying the "filter coefficient" η_n by $2\pi/\Delta t$ yields the value of $h(n\Delta t)$.

The Parks-McClellan code is unreliable when it tries to find approximating polynomials of degree greater than 25 or so. However, it has no problems with *trigonometric* polynomials of degree 500 (!). This phenomenon can ultimately be traced to the stability of the discrete Fourier transform (a unitary transformation), which would be a strong competitor to the best approximating polynomial.

As an example of the efficacy of this procedure, consider an industry standard for a resampler, the Intersil #216 interpolator, which is designed for operation with 50% oversampling. The support of the interpolating kernel $h_{\#216}(t)$ has length 6, and it interpolates 32 values per sampling interval. Its signal-to-noise ratio in the passband is 30 dB, and its SFDR is 62 dB.

Requesting a $6 \times 32 = 192$-degree trigonometric polynomial from MATLAB's remez.m m-file with passband/stopband weights in the ratio 1:290, we computed an interpolating kernel with the same support as #216 that achieved an inband accuracy SNR of 30 dB and a SFDR of 79 dB - an enormous improvement, achieved simply by altering the stored values of $h(t)$ (!) The interpolating kernel $h(t)$ is shown in Figure 2 and its Fourier transform in Figure 10.

We also designed an interpolating kernel of support length 8 achieving 30 dB SNR, 100 dB SFDR at 50% oversampling, and one of support length 18 achieving 30 dB SNR, 100 dB SFDR at only 20% oversampling. Their transforms are displayed in Figures 11 and 12.

V. REMARKS

A. Farrow's Scheme

The interpolating kernel $h(t)$ is, of course, computed in tabulated form, and can be stored as a table. In fact, this format is used in the Intersil #216. Farrow [8] has proposed a very systematic implementation of the resampling calculations if $h(t)$ is stored as a (true) polynomial. We have concatenated the trigonometric-polynomial Remez algorithm described above with the Remez best-(true)-polynomial fitter to achieve this.

For an oversampling margin of 50%, the degree-28 polynomial approximant to the interpolating kernel $h(t)$ in $Fig.$ $1b$ (support length $=$ 6, SNR $=$ 30 dB, SFDR $=$ 79 dB,) achieves comparable SNR and SFDR levels (30 and 77 dB); lower degree approximants cannot match this SFDR performance. For the kernel of support length 8, which achieved 100 dB SFDR, its degree-28 approximant delivers 93 dB SFDR. Finding a polynomial approximant for the kernel of support length 18, which achieved 100 dB SFDR at 20% oversampling, was impossible; a degree-33 approximant delivered only 51 dB, and higher degree polynomials were illconditioned. This highlights the difference between trigonometric and true polynomial approximants; the trigonometric polynomial which comfortably generated this h(t) has degree 576 (!)
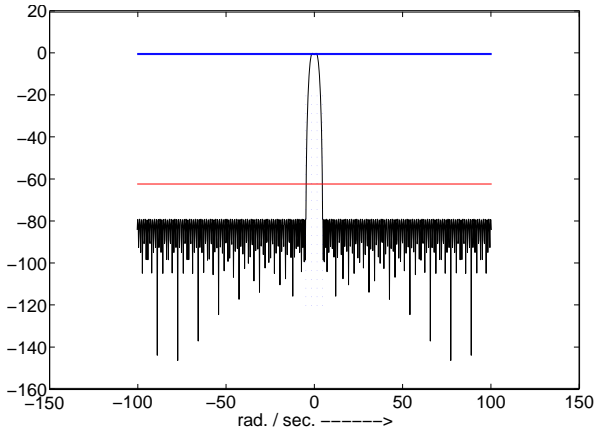
Fig. 10. 6-tap re-sampler: $2\pi H(\omega T)$
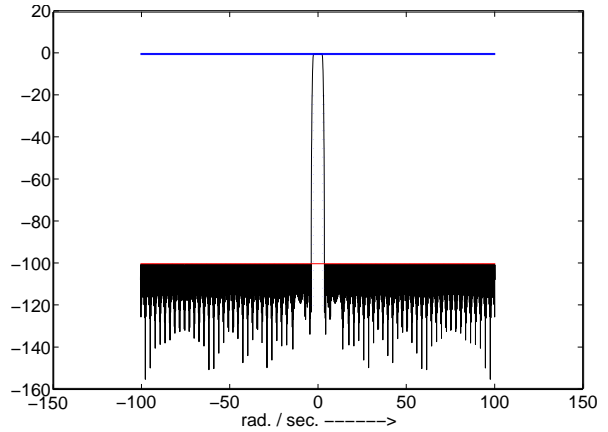
Fig. 12. 18-tap re-sampler: $2\pi H(\omega T)$
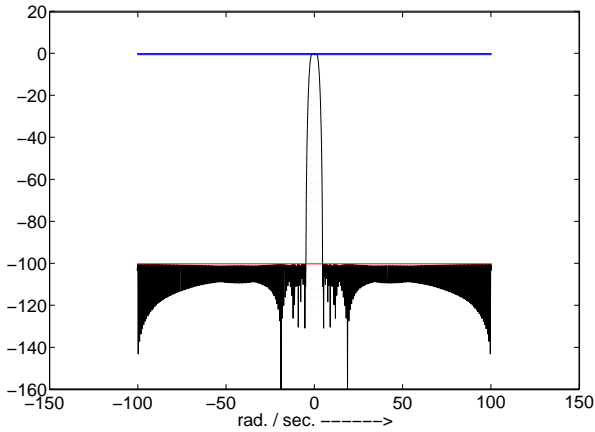
Fig. 11. 8-tap Re-sampler: $2\pi H(\omega T)$

Of course, the Farrow scheme sacrifices speed of computation for reduced memory requirements. A variant of the Farrow scheme can be constructed to employ piecewise polynomial interpolating kernels. We constructed an approximant to the kernel of support length 8 (30 dB SNR, 100 dB SFDR) consisting of 8 degree-6 polynomials that delivered 30 dB SNR and 94 dB SFDR.

B. Complexity

The storage of tabulated values of $h(t)$ or of its polynomial approximants is facilitated by symmetry; both are even functions. Piecewise polynomial approximants do not enjoy this property. The evaluation of equation (2) requires one multiply per unit length of the support of $h(t)$, times the computational burden of evaluating each value of $h(t)$ - zero for tabulated values, d multiplies for piecewise polynomials of degree d (Horner's method), $[d/2 + 1]$ multiplies for full polynomials (half the degree for even polynomials plus one to calculate t^2).

C. Jitter

Jitter is the phenomenon that occurs due to imprecise stipulation of the interpolation time t (due to discretization,

rounding, etc.) We estimated this effect by comparing the SNRs and SFDRs reported for a discretization level of 32 points per unit time with those for 128 points. The discrepancies only amounted to fractions of dB.

D. Inband Error Metrics

The common industry practice for estimating the accuracy of the interpolates is the ratio of the signal noise (L_2 norm squared) to the error noise, equation (7). Other norm-estimates can be similarly derived. Among the possibilities are the following:

$$N \leq 2\pi \max \left|X(\omega)\right|^2 \int_{-\Omega_{BW}}^{\Omega_{BW}} \left|1 - 2\pi H(\omega T)\right|^2 d\omega,$$

$$\leq \left\|x(t)\right\|_1^2 \int_{-\Omega_{BW}}^{\Omega_{BW}} \left|1 - 2\pi H(\omega T)\right|^2 d\omega \, /2\pi,$$

$$= \left\|x(t)\right\|_1^2 \left\|sinc(t) - h(t)\right\|_2^2,$$

E. Filter interpretations

A filter equation has the form $z(t) = \sum_n y(t - n)h(n)$. The interpolator equation (2) does not qualify, because of the variability of the parameter τ in the argument of h (in the right hand member of (2)). If $\tau = $ constant, however, (2) is a filter, and it should therefore have sinusoids as eigenfunctions; it follows that the complex monotone $e^{j\Omega T}$ is an eigenfunction and should be reproduced without spurs. This is, in fact, the case because the signal is then resampled at the same frequency; all the spurs align in Figure 6, for $T' = T$.

Another interpretation of equation (2) that validates it as a filter equation is seen by subdividing the sample interval $T = P\Delta t$, taking $t = n\Delta t$, and defining the discrete signal $x_{sample}(n\Delta t) = x(\frac{n}{P}T)$ when $\frac{n}{P}$ is an integer, 0 otherwise; for then (2) becomes

$$\xi(m\Delta t) = \sum_k x_{samp}(k\Delta t) \, h(\frac{k - m}{P}),$$

which has the filter format. All the frequency interpretations described above can be gleaned from this formulation.

Before we happened upon the notion of attacking the problem with the Remez algorithm, we expended (a lot of) effort to design interpolating kernels $h(t)$ with small supports by using classical windowing functions to approximate the "boxcar" transform of the sinc function. We tested iterated Hamming windows, combination of Helms-Thomas [9, 10] and Hamming windows, and C^∞-mollified boxcars to try to bring the SFDR down. While we successfully achieved rapid falloff of $H(\omega)$ for large $|\omega|$, the thorny first spur at $\omega \approx 2\pi/T - \Omega_{BW}$ (Figure 5) was impossible to suppress. The equiripple structure, exhibited in Figure 9, of the Fourier transforms of the interpolating transforms produced by our new procedure provides the "flat" falloff that is needed. Indeed, it shows that the new kernels are optimal in the usual sense [11].

VI. Conclusion

This novel application of the Remez algorithm handsomely outperforms all of the interpolators surveyed by the authors when the SFDR is taken into consideration. It seems likely that it will prove to be optimal for the resampling task. Codes for designing these resamplers for arbitrary system specifications are available from the second author (patent pending).

References

[1] J. R. Higgins, "Five Short Stories About the Cardinal Series," *Bull. Amer. Math. Soc.*, vol. 12, no. 1, pp. 45-89, 1985.

[2] P. L. Butzer, W. Splettstosser and R. L. Stens, "The Sampling Theorem and Linear Prediction in Signal Analysis," *Jber. d. Dt. Math.-Verein.* vol. 90, pp. 1-70, 1988.

[3] P. L. Butzer and R. L. Stens, "Sampling Theory for Not Necessarily Band-Limited Functions: A Historical Review" *SIAM Rev.*, vol. 34, no. 1, pp. 40-53, 1992.

[4] A. G. Garcia, "Orthogonal Sampling Formulas: A Unified Approach," *SIAM Rev.*, vol. 42, no. 3, pp. 499-512, 2000.

[5] A. J. Jerri, "The Shannon Sampling theorem - Its Various Extensions and Applications: a Tutorial Review," *Proc. IEEE*, vol. 65, no. 11, pp. 1565-1596, 1977.

[6] M. Unser, "Sampling - 50 Years After Shannon," *Proc. IEEE,* vol. 88, no. 4, pp. 569-587, April 2000.

[7] A. I. Zayed, *Advances in Shannon's Sampling Theorem*, Boca Raton, FL: CRC Press, 1993.

[8] C. W. Farrow, "A Continuously Variable Delay Element," *ISCAS '88*, IEEE 1988.

[9] H. D. Helms and J. B. Thomas, "Truncation Error of Sampling-Theorem Expansions," *Proc. IRE*, vol. 50, pp. 179-184, Feb. 1962.

[10] D. Jagerman, "Bounds for Truncation Error of the Sampling Expansion," *SIAM J. App. Math.*, vol. 14, no. 4, pp. 714- 723, July 1966.

[11] L. J. Karam and J. H. McClellan, "Complex Chebychev Approximation for FIR Filter Design," *IEEE Trans. Circ. & Syst.*, vol. 42, no. 3, pp. 207-215, March 1995.